Effects of Temperature and Biodiesel Fraction on Densities of Commercially Available Diesel Fuel and Its Blends with the Highest Methyl Ester Yield Corn Oil Biodiesel Produced by Using NaOH

Atilla Bilgin and Mert Gülüm

1 Introduction

Diesel engines are being extensively utilized in a number of sectors such as road and train transport, agriculture, military, construction, mining, and stationary electricity production in the world (Esteban et al. 2012). They have appealing features including robustness, higher torque, and lower fuel consumption under certain conditions (Esteban et al. 2012). Diesel engines can use many fuels such as light and heavy diesel fuels, straight vegetable oils (SVO), kerosene, gas fuels, short-chain alcohols, and biodiesel (Esteban et al. 2012; Iwasaki et al. 1995). Biodiesel is described as a fuel comprising mono-alkyl esters of long-chain fatty acids (FA) derived from vegetable oils or animal fats (Yuan et al. 2005). It is usually produced through transesterification reaction, either under low-temperature heterogeneous conditions using alkaline, acid, enzyme, or heterogeneous solid catalysts or under high-temperature (usually $> 250\ ^{\circ}C$) homogeneous conditions without using any catalyst (Lin et al. 2014). Biodiesel is receiving increasing attention day by day (Canakci 2007) because of its many great benefits over diesel fuel as following: (1) it is renewable (Yuan et al. 2009), biodegradable (Mejia et al. 2013), and a non-toxic fuel (Ozcanli et al. 2012); (2) it has a higher cetane number than diesel fuel and contains about 10–11% oxygen by mass in the molecular structure, thus improving combustion efficiency and reducing the emission of carbon monoxide (CO), un-burnt hydrocarbons (HCs), and particulate matter (PM) in exhaust emissions (Canakci 2007); (3) it has a higher flash point temperature, making its handling, use, and transport safer than diesel fuel (Gaurav et al. 2013); (4) it

A. Bilgin (✉) • M. Gülüm
Karadeniz Technical University, Faculty of Engineering, Mechanical Engineering Department, Trabzon 61080, Turkey
e-mail: bilgin@ktu.edu.tr

F. Aloui, I. Dincer (eds.), *Exergy for A Better Environment and Improved Sustainability 2*, Green Energy and Technology,
https://doi.org/10.1007/978-3-319-62575-1_5

improves lubricity and reduces premature wearing of fuel pumps (Stalin and Prabhu 2007); (5) the use of biodiesel can help reduce the world's dependence on fossil fuels because biodiesel can be produced by using domestic renewable feedstock (Basha and Gopal 2012); and (6) it can be completely miscible with diesel fuel in any proportion because of the similar chemical structures of these two fuels. Although these properties make it an ideal fuel for diesel engines, it also has some disadvantages such as higher feedstock cost and NO_x exhaust emissions in some cases, inferior storage and oxidative stability, and lower energy content (Rahimi et al. 2014; Sivanathan and Chandran 2014; Moser 2012).

As the use of biodiesel has become more widespread, researchers have shown a strong interest in modeling the combustion process in order to understand the fundamental characteristics of biodiesel combustion (Yuan et al. 2003). They often use the physical properties of biodiesel as input data in their combustion models for the computational softwares (KIVA, Fluent, and AVL Fire). However, it may not be practical at every turn to make measurements of physical properties of biodiesel or biodiesel–diesel fuel blends for each blending ratio or temperature in any study. Regression models as a function of temperature, percentage of blend, and chemical structure have been generally used to calculate these properties without measurements. Some studies reporting these models are summarized as follows. Sivaramakrishnan and Ravikumar (2011) developed an equation depending on kinematic viscosity, density, and flash point temperature for estimating higher heating values (HHV) of methyl esters of various vegetable oils. The equation was able to predict HHV with 0.949 accuracy. Pratas et al. (2011) measured densities of various biodiesels in the temperature range of 273–363 K at atmospheric pressure. Three versions of Kay's mixing rules and two versions of the group contribution method for predicting saturated liquid (GCVOL) models were derived by using experimental data in this study. Tong et al. (2011) presented the relationship between cetane number of pure biodiesel and FAME composition (carbon number of fatty acid chain) by developing a linear regression. According to results, the linear equation showed excellent correlation with $R^2 = 0.9904$ and a maximum average absolute error of 0.49.

The present chapter deals with the investigation of the effects of biodiesel fraction in blend (X) and temperature (T) on densities of the highest methyl ester content corn oil biodiesel (B100) and its blends (B5, B15, B20, and B25) with commercially available diesel fuel (D). Some new one- and two-dimensional models were also derived for predicting the densities of biodiesel–diesel fuel blends, and these models were compared with other equations published in the literature.

Nomenclature

$a, b, c, d \ldots, g$	Regression constants
B5,B10,B15,B20	Biodiesel–diesel fuel blends
B100	Pure corn oil biodiesel
D	Pure diesel fuel
HHV	Higher heating value (kJ/kg)

(continued)

K_{ball}	Coefficient of the viscometer ball (mPa·s·cm^3/g/s)
m_{total}	Mass of the pycnometer filled with biodiesel (g)
R	Correlation coefficient
t	Falling time of the viscometer ball (s)
T	Temperature ($^\circ$C)
$w_1, w_2, w_3, \ldots, w_n$	Uncertainties of independent variables
$x_1, x_2, x_3, \ldots, x_n$	Independent variables
X	Biodiesel fraction in blend (%)
Greek letters	
μ	Dynamic viscosity (cP ≡ mPa.s)
ν	Kinematic viscosity (cSt ≡ mm^2/s)
ρ	Density (kg/m^3), (g/cm^3)

2 Experimental Methods

2.1 Biodiesel Production

In this study, commercially available refined corn oil was used for biodiesel production. There was no need to perform a pretreatment to the oil because the oil was refined. Methanol (CH_3OH) of 99.8% purity as alcohol and pure-grade sodium hydroxide (NaOH) as a catalyst were used in the transesterification reaction. To produce corn oil biodiesel having the highest methyl ester yield, optimum reaction parameters were 0.90% catalyst concentration (mass of NaOH/mass of corn oil), 50 $^\circ$C reaction temperature, 60 min reaction time, and 6:1 alcohol/oil molar ratio, as given by Gülüm (2014). The transesterification reaction was carried out in a 1-L flat-bottomed flask, equipped with a magnetic stirrer heater, thermometer, and spiral reflux condenser. Haake falling ball viscometer, Isolab pycnometer, top loading balance with an accuracy of 0.01 g, Haake water bath, and a stopwatch with an accuracy of 0.01 s were used to measure dynamic viscosity and density. Before starting the reaction, the catalyst was dissolved in methanol to make an alcoholic solution of the catalyst in a narrow-neck flask. In the flat-bottomed flask, the alcoholic solution was added to the 200 g of corn oil that was formerly warmed to about 80 $^\circ$C in a beaker. These reactants were mixed with a stirring speed of 500 rpm using the magnetic stirrer heater. The transesterification reaction was carried out with the spiral reflux condenser for avoiding loss of alcohol. Also, reaction temperature was controlled using a thermometer to remain constant during the reaction. At the end of reaction, the resulting products mixture was transferred to a separating funnel. After a day, two phases formed in the separating funnel. The upper phase consisted of methyl esters (biodiesel), while the lower one consisted of glycerol, excess methanol, and the remaining catalyst together with soap. After separation of the two layers by gravity, the biodiesel phase was washed with warm

distilled water until the water became clear. The washed biodiesel was heated up to about 100 °C to remove methyl alcohol and water residuals.

2.2 Density Measurements

The densities of the produced biodiesel and its blends were determined by means of Eq. (1) and measurements in accordance with ISO 4787 standard:

$$\rho_{\text{blend}} = \frac{m_{\text{total}} - m_{\text{pycnometer}}}{m_{\text{water}}} \rho_{\text{water}} \tag{1}$$

where ρ and m represent density and mass, respectively. In order to minimize measurement errors, all measurements were conducted three times for each sample and the results were averaged. Also, an uncertainty analysis was carried out, depending on the sensitivities of measurement devices.

2.3 Dynamic Viscosity Measurement

The dynamic viscosities were determined in accordance with DIN 53015 standard using Eq. (2) and making measurements by means of the Haake falling ball viscometer, Haake water bath, and stopwatch:

$$\mu_{\text{blends}} = K_{\text{ball}}(\rho_{\text{ball}} - \rho_{\text{blends}})t \tag{2}$$

where μ is dynamic viscosity, K_{ball} is coefficient of the viscometer ball, and t is falling time of the ball moving between two horizontal lines marked on the viscometer tube at limit velocity. K_{ball} and ρ_{ball} are 0.057 mPa·s·cm^3/g/s and 2.2 g/cm^3, respectively.

The kinematic viscosities were determined from Eq. (3) by dividing dynamic viscosity to density at the same temperature:

$$\nu_{\text{blend}} = \frac{\mu_{\text{blend}}}{\rho_{\text{blend}}} \tag{3}$$

In Eq. (3), if $\mu_{\text{biodiesel}}$ and ρ_{biodisel} are in the unit of (cP) and (kg/L), respectively, then $\nu_{\text{biodiesel}}$ is obtained in the unit of cSt.

In this study, dynamic and kinematic viscosities and densities were measured in the Internal Combustion Engines Laboratory in the Mechanical Engineering Department at Karadeniz Technical University. The fatty acid methyl esters of the produced corn oil biodiesel were qualitatively and quantitatively analyzed by gas chromatography using a Hewlett-Packard HP-6890 Series GC system fitting

Table 1 Some fuel properties of diesel fuel, produced biodiesel and their blends, and corresponding standard values for biodiesel

Properties	Unit	D	B5	B10
Viscosity at 40 °C	cSt	2.700	3.154	3.332
Density at 15 °C	kg/m^3	832.62	835.47	838.11
Flash point	°C	63	70	76
HHV	kJ/kg	45950	45632	45359

B15	B20	B100	EN14214	ASTM-D6751
3.658	3.865	4.137	3.50–5.00	1.90–6.00
839.13	842.18	882.07	860–900	[a]
80	88	173	101≤	130≤
45051	44758	39981	[a]	[a]

[a]Not specified

Table 2 Fatty acid methyl ester composition of the produced biodiesel

Fatty acid	Mass, %
Palmitic (C16:0)	15.776
Oleic (C18:1)	47.703
Linoleic (C18:2)	33.415
α-Linolenic acid (C18:3)	1.101
Arachidic (C20:0)	0.805
Gadoleic acid (C20:1)	0.493
Behenic (C22:0)	0.347
Lignoceric (C24:0)	0.359
Average molecular mass	292.561 g/mol[a]
Typical formula	$C_{18.74}H_{35.12}O_2$[a]

[a]Calculated from fatty acid distribution

with a HP-6890 mass selective detector (1909N-133 innowax capillary column of 30 m length, 0.25 mm I.D, and 0.25 μm film thickness) in the Science Research and Application Center at Mustafa Kemal University. The other properties of the pure fuels and fuel blends such as flash point temperature (EN ISO 3679) and higher heating value (DIN 51900-2) were measured at the Prof. Dr. Saadettin GÜNER Fuel Research and Application Center at Karadeniz Technical University. These properties and EN 14214 and ASTM D 6751 standard values are given in Table 1. Also, the fatty acid compositions of the produced corn oil biodiesel and its calculated average molecular mass and typical formulae are given in Table 2.

2.4 Uncertainty Analysis

The results obtained from experimental studies are generally calculated from measured physical quantities. These quantities have some uncertainties due to uncertainties of measuring tools and measurement systems. Therefore, uncertainty

analysis should be applied for proving reliability of the calculated results. In this study, uncertainties of the measured and calculated physical quantities such as dynamic and kinematic viscosities and density values were determined by the method proposed by Holman (2001). According to this method, if the result R is a given function of the independent variables $x_1, x_2, x_3, ..., x_n$ and $w_1, w_2, w_3, \ldots, w_n$ are the uncertainties of each independent variable, then the uncertainty of the result w_R is calculated by using the equation:

$$w_R = \left[\left(\frac{\partial R}{\partial x_1} \cdot w_1 \right)^2 + \left(\frac{\partial R}{\partial x_2} \cdot w_2 \right)^2 + \ldots + \left(\frac{\partial R}{\partial x_n} \cdot w_n \right)^2 \right]^{1/2} \quad (4)$$

According to Eq. (4), the highest uncertainty was determined as 0.0364%. Therefore, it can be said that the results have fairly high reliability.

3 Results and Discussions

3.1 One-Dimensional Linear Models

3.1.1 Effects of Biodiesel Fraction on Density

The variations of densities of fuel blends (B5, B10, B15, and B20) with respect to biodiesel fractions (X) for different temperatures (T) are shown in Fig. 1. In this

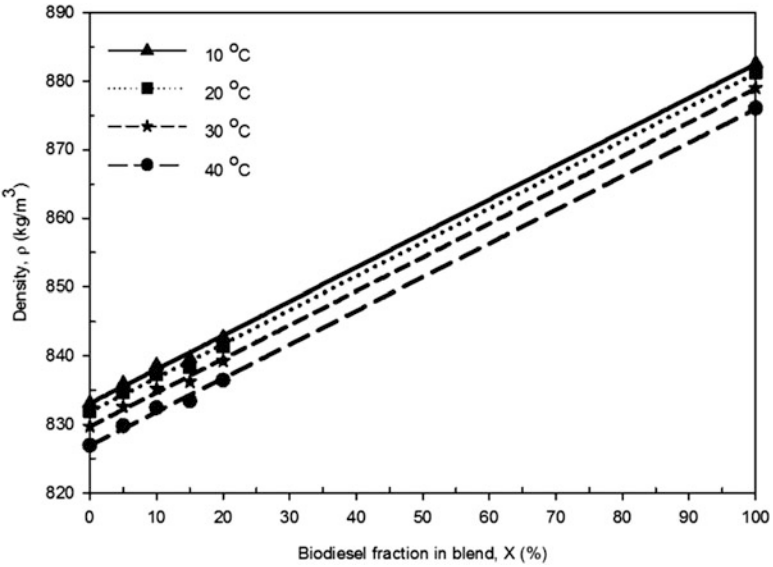

Fig. 1 Changes of density values of fuel blends with respect to biodiesel fraction for various temperatures

figure, the points correspond to measured density values at studied temperatures and biodiesel fractions, while the lines are plots of a curve-fit equation. As well-known, densities increase with increase in biodiesel fraction for a specific temperature, and these are directly proportional to biodiesel content. For these reasons, the linear model, given in Eq. (5), is fitted to the measured data:

$$\rho = \rho(X) = a + bX \tag{5}$$

where ρ is density of the blends in kg/m^3 and a and b are regression constants.

The measured and calculated density values from Eq. (5), error rates between measured and calculated values, regression constants, and correlation coefficients (R) are given in Table 3. The correlation coefficient is a quantitative measure of goodness of fit of the regression equation to the measured data. For a perfect fit, for example, R becomes 1, which means that the equation explains 100% of the

Table 3 The measured densities, calculated densities from Eq. (5), error rates between measured and calculated densities, regression constants, and correlation coefficients for different temperatures

	Measured, ρ(kg/m^3)					
	Blend, X(%)					
Temp. T($^\circ$C)	0	5	10	15	20	100
10	833.12	835.97	838.62	839.63	842.69	882.60
20	831.87	834.71	837.36	838.37	841.42	881.28
30	829.74	832.58	835.22	836.23	839.27	879.03
40	826.95	829.78	832.41	833.42	836.45	876.07

Regression constants		
a	b	R
833.1000	0.4941	0.9996
831.8000	0.4934	0.9996
829.7000	0.4922	0.9996
826.9000	0.4905	0.9996

Calculated, ρ(kg/m^3)					
Blend, X(%)					
0	5	10	15	20	100
833.1000	835.5705	838.0410	840.5115	842.9820	882.5100
831.8000	834.2670	836.7340	839.2010	841.6680	881.1400
829.7000	832.1610	834.6220	837.0830	839.5440	878.9200
826.9000	829.3525	831.8050	834.2575	836.7100	875.9500

Relative error rates (%)					
Blend, X(%)					
0	5	10	15	20	100
0.0024	0.0478	0.0690	0.1050	0.0347	0.0102
0.0084	0.0531	0.0748	0.0991	0.0295	0.0159
0.0048	0.0503	0.0716	0.1020	0.0326	0.0125
0.0060	0.0515	0.0727	0.1005	0.0311	0.0137

variability of the measured data (Chapra and Canale 1998). All correlation coefficients and the maximum relative error rate for B15 blend were obtained as 0.9996 and 0.1050%, respectively. These results and Fig. 1 show that the linear model yields the excellent agreement between measured and calculated density values, as expected.

3.1.2 Effects of Temperature on Density

Figure 2 presents the effects of temperature on densities of pure fuels and biodiesel–diesel fuel blends. As shown in the figure, the densities, as expected, decrease with increasing temperature and there are similar trends for all fuels and blends in the studied temperature range. The distributions of densities with temperature were correlated with the following linear and power models:

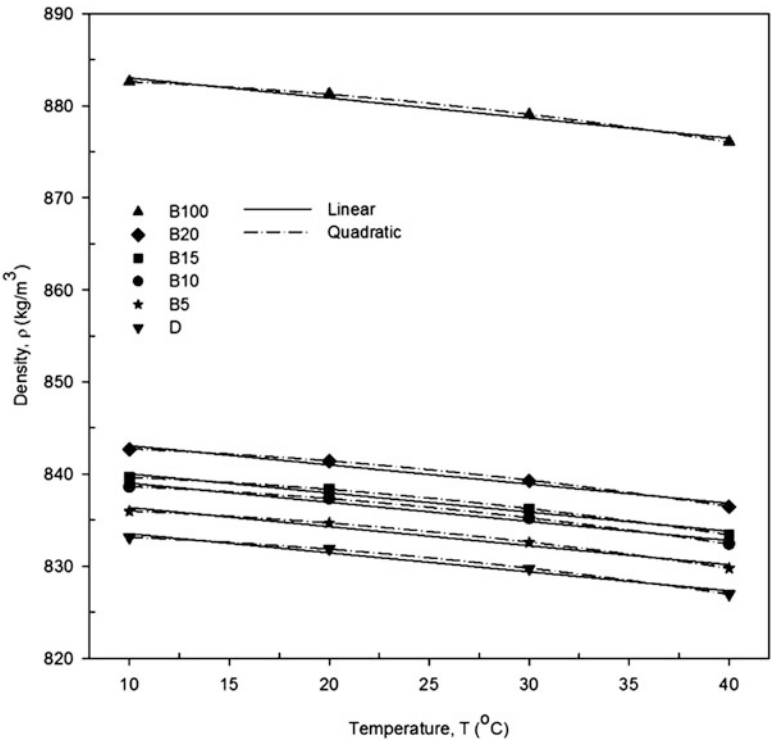

Fig. 2 Variations of density values of pure fuels and fuel blends with respect to temperature for different regression models

The linear model:

$$\rho = \rho(T) = a + bT \tag{6}$$

The power model:

$$\rho = \rho(T) = aT^b + c \tag{7}$$

where T is temperature in $^{\circ}$C and a, b, and c are regression constants.

Tables 4 and 5 list the measured and calculated (from Eqs. (6) and (7)) densities of the blends and pure fuels, error rates between them, regression constants, and correlation coefficients. For linear and power models, the maximum relative error rates were computed as 0.0539% and 0.0002%, respectively. The R values are between 0.9862 and 0.9865 for the linear model, while they all have a value of 0.9999 for the power model. According to these results, the power model as a function of T has higher accuracy in calculating densities of fuels and blends.

3.2 Two-Dimensional Surface Models

In this study, two-dimensional surface models were also improved to make quick estimates of densities for a given X and a specific T simultaneously. As mentioned previously, there was a linear relationship between density and biodiesel fraction, while linear and power models were tried to represent changes of densities with temperature, which may have non-linear characteristics. In the light of this knowledge, the experimental density values were correlated using new two-dimensional surface models represented as following:

The linear surface model:

$$\rho = \rho(T, X) = a + bT + cX \tag{8}$$

The model linear with respect to X and power with respect to T:

$$\rho = \rho(T, X) = aT^b + cX \tag{9}$$

where ρ is density in (kg/m^3) and a, b, and c are regression constants.

Tables 6 and 7 show the regression constants, measured densities, calculated densities from Eqs. (8) and (9), relative error rates between them, and correlation coefficients. The maximum relative error rates and R values from Eqs. (8) and (9) are 0.1506%, 0.1867% and 0.9993, 0.9983, respectively. These results indicate that variations of densities with X and T simultaneously are observed to be well correlated by the linear surface model.

Figures 3 and 4 depict plots of changes of constant density lines for fuel blends as functions of T and X calculated from these models. According to linear surface model by which changes of densities are well correlated, because the change of

Table 4 The measured densities, calculated densities from Eq. (6), error rates between measured and calculated densities, regression constants, and correlation coefficients for different biodiesel fractions

Blend X(%)	Measured, ρ(kg/m^3) Temp., T(°C)			
	10	20	30	40
0	833.12	831.87	829.74	826.95
5	835.97	834.71	832.58	829.78
10	838.62	837.36	835.22	832.41
15	839.63	838.37	836.23	833.42
20	842.69	841.42	839.27	836.45
100	882.60	881.28	879.03	876.07

Regression constants		
a	B	R
835.6000	−0.2064	0.9863
838.4000	−0.2070	0.9864
841.1000	−0.2077	0.9863
842.1000	−0.2077	0.9863
845.2000	−0.2087	0.9865
885.2000	−0.2184	0.9862

Calculated, ρ(kg/m^3) Temp., T(°C)			
10	20	30	40
833.5360	831.4720	829.4080	827.3440
836.3300	834.2600	832.1900	830.1200
839.0230	836.9460	834.8690	832.7920
840.0230	837.9460	835.8690	833.7920
843.1130	841.0260	838.9390	836.8520
883.0160	880.8320	878.6480	876.4640

Relative error rates (%) Temp., T(°C)			
10	20	30	40
0.0499	0.0478	0.0400	0.0476
0.0431	0.0539	0.0468	0.0410
0.0481	0.0494	0.0420	0.0459
0.0468	0.0506	0.0432	0.0446
0.0502	0.0468	0.0394	0.0481
0.0471	0.0508	0.0435	0.0450

density with respect to both temperature and biodiesel fraction is linear, the constant density lines become linear in characteristic and have constant gradients, as shown in Fig. 3. Therefore, if temperature is changed in a unit amount, in order to keep the density of the fuel blend constant, the temperature change should be multiplied by a factor corresponding to the slope of the constant density line, i.e., to change the biodiesel fraction in the blend.

Table 5 The measured densities, calculated densities from Eq. (7), error rates between measured and calculated densities, regression constants, and correlation coefficients for different biodiesel fractions

Blend X(%)	Measured, ρ(kg/m^3) Temp., T(°C) 10	20	30	40
0	833.12	831.87	829.74	826.95
5	835.97	834.71	832.58	829.78
10	838.62	837.36	835.22	832.41
15	839.63	838.37	836.23	833.42
20	842.69	841.42	839.27	836.45
100	882.60	881.28	879.03	876.07

Regression constants			
a (10^{-3})	B	c	R
−5.5610	1.9210	833.6000	0.9999
−5.6270	1.9190	836.4000	0.9999
−5.5860	1.9220	839.1000	0.9999
−5.5860	1.9220	840.1000	0.9999
−5.7140	1.9170	843.2000	0.9999
−5.7370	1.9280	883.1000	0.9999

Calculated, ρ(kg/m^3) Temp., T(°C) 10	20	30	40
833.1364	831.8444	829.7744	826.9517
835.9330	834.6342	832.5552	829.7223
838.6332	837.3312	835.2441	832.3971
839.6332	838.3312	836.2441	833.3971
842.7280	841.4176	839.3222	836.4689
882.6139	881.2504	879.0582	876.0619

Relative error rates (%) Temp., T(°C) 10	20	30	40
0.0020	0.0031	0.0041	0.0002
0.0044	0.0091	0.0030	0.0070
0.0016	0.0034	0.0029	0.0015
0.0004	0.0046	0.0017	0.0027
0.0045	0.0003	0.0062	0.0023
0.0016	0.0034	0.0032	0.0009

Table 6 The measured densities, calculated densities from Eq. (8), error rates between measured and calculated densities, regression constants, and correlation coefficient for different biodiesel fractions and temperatures

Temp. $T(^{\circ}C)$	Blend $X(\%)$	Measured $\rho(kg/m^3)$	Calculated $\rho(kg/m^3)$	Relative error rates (%)
10	0	833.12	833.5070	0.0465
	5	835.97	835.9695	0.0001
	10	838.62	838.4320	0.0224
	15	839.63	840.8945	0.1506
	20	842.69	843.3570	0.0792
	100	882.60	882.7570	0.0178
20	0	831.87	831.4140	0.0548
	5	834.71	833.8765	0.0999
	10	837.36	836.3390	0.1219
	15	838.37	838.8015	0.0515
	20	841.42	841.2640	0.0185
	100	881.28	880.6640	0.0699
30	0	829.74	829.3210	0.0505
	5	832.58	831.7835	0.0957
	10	835.22	834.2460	0.1166
	15	836.23	836.7085	0.0572
	20	839.27	839.1710	0.0118
	100	879.03	878.5710	0.0522
40	0	826.95	827.2280	0.0336
	5	829.78	829.6905	0.0108
	10	832.41	832.1530	0.0309
	15	833.42	834.6155	0.1434
	20	836.45	837.0780	0.0751
	100	876.07	876.4780	0.0466

Regression constants	Correlation coefficient
$a = 835.6000$	$R = 0.9993$
$b = -0.2093$	
$c = 0.4925$	

4 Conclusions

In this chapter, the effects of biodiesel fraction and temperature on the densities of the highest methyl ester content corn oil biodiesel and its blends with commercially available diesel fuel were investigated. One- and two-dimensional regression models were also developed to predict the densities of the pure fuels and blends at different temperatures. The following conclusions can be drawn from this study:

Table 7 The measured densities, calculated densities from Eq. (9), error rates between measured and calculated densities, regression constants, and correlation coefficient for different biodiesel fractions and temperatures

Temp. $T(^{\circ}C)$	Blend $X(\%)$	Measured $\rho(kg/m^3)$	Calculated $\rho(kg/m^3)$	Relative error rates (%)
10	0	833.12	833.8099	0.0828
	5	835.97	836.2724	0.0362
	10	838.62	838.7349	0.0137
	15	839.63	841.1974	0.1867
	20	842.69	843.6599	0.1151
	100	882.60	883.0599	0.0521
20	0	831.87	830.8555	0.1220
	5	834.71	833.3180	0.1668
	10	837.36	835.7805	0.1886
	15	838.37	838.2430	0.0152
	20	841.42	840.7055	0.0849
	100	881.28	880.1055	0.1333
30	0	829.74	829.1321	0.0733
	5	832.58	831.5946	0.1184
	10	835.22	834.0571	0.1392
	15	836.23	836.5196	0.0346
	20	839.27	838.9821	0.0343
	100	879.03	878.3821	0.0737
40	0	826.95	827.9115	0.1163
	5	829.78	830.3740	0.0716
	10	832.41	832.8365	0.0512
	15	833.42	835.2990	0.2255
	20	836.45	837.7615	0.1568
	100	876.07	877.1615	0.1246

Regression constants	Correlation coefficient
$a = 843.7000$	$R = 0.9983$
$b = -0.005121$	
$c = 0.4925$	

- In linear models, the linear and power ones were quite suitable to represent density–biodiesel fraction and density–temperature variations, respectively. Correlation coefficients (R) and maximum relative error rates were determined as 0.9996, 0.1050% and 0.9999, 0.0002% for the linear and power models, respectively.
- Two-dimensional linear surface model with the correlation coefficient of 0.9993 showed the higher degree of accuracy for representing the change in density with temperature and biodiesel fraction in the blend simultaneously. Maximum

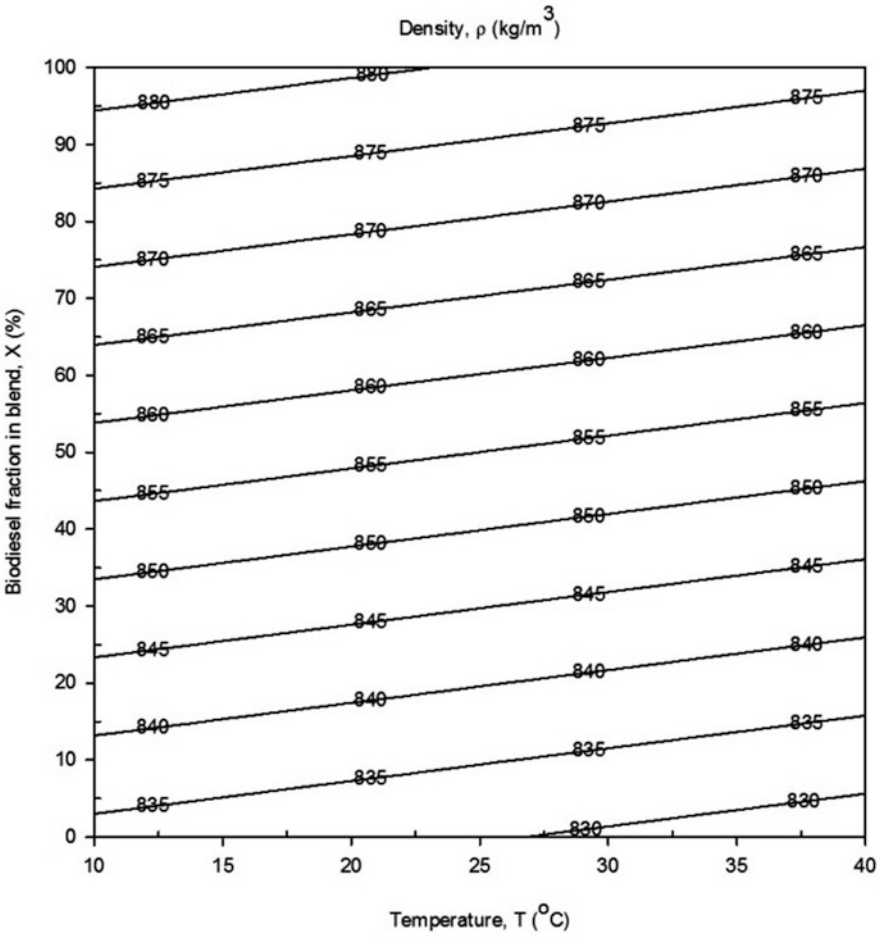

Fig. 3 Variations of constant density lines of fuel blends as functions of temperature and biodiesel fraction simultaneously calculated from Eq. (8)

relative error rate between the measured and calculated density values were computed as 0.1506% for this model.

- The two-dimensional constant density line plot obtained by the linear surface model has constant gradients, as shown in Fig. 3. This means that when temperature is changed in a unit amount, the temperature change should be multiplied by a factor corresponding to the slope of the constant density line for keeping the density of the fuel blend constant.

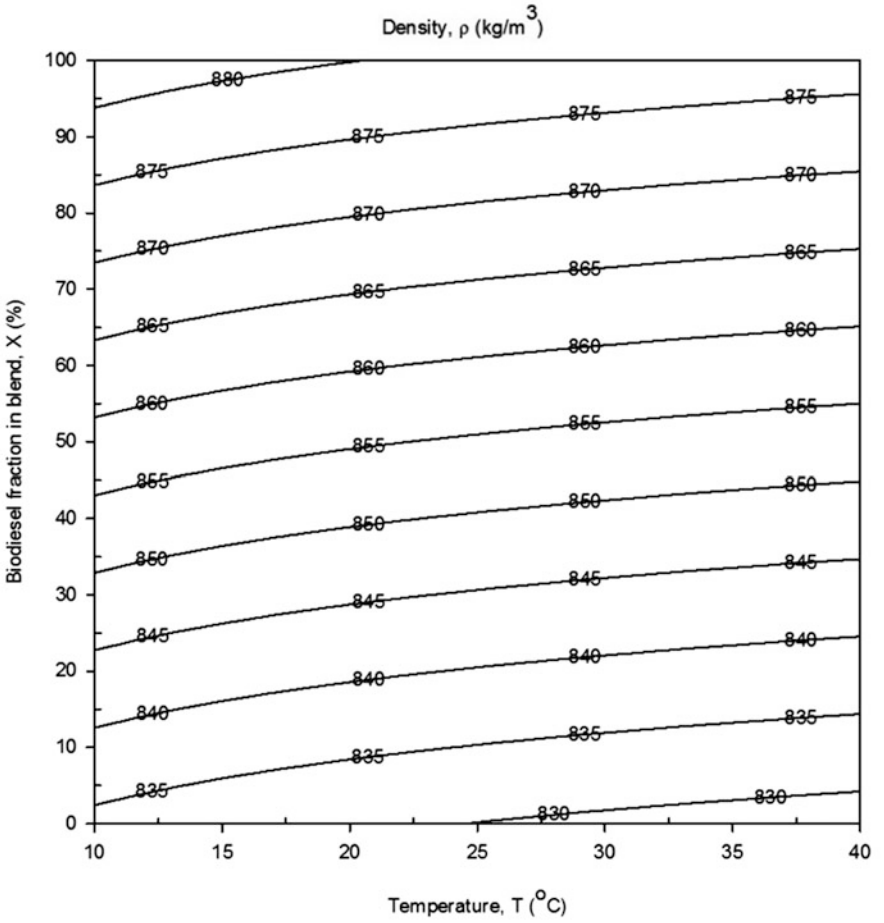

Fig. 4 Variations of constant density lines of fuel blends as functions of temperature and biodiesel fraction simultaneously calculated from Eq. (9)

Acknowledgments The authors express their gratitude to Karadeniz Technical University Scientific Research Projects Fund for financial support received (Project No: 9745).

References

Basha, S.A., Gopal, K.R.: A review of the effects of catalyst and additive on biodiesel production, performance, combustion and emission characteristics. Renew. Sust. Energ. Rev. **16**, 711–717 (2012)

Canakci, M.: Combustion characteristics of a turbocharged DI compression ignition engine fueled with petroleum diesel fuels and biodiesel. Bioresour. Technol. **98**, 1167–1175 (2007)

Chapra, S.C., Canale, P.R.: Numerical Methods for Engineers with Software and Programming Applications, 3rd edn. Mc-Graw-Hill, New York (1998)
Esteban, B., Riba, J.R., Baquero, G., Rius, A., Puig, R.: Temperature dependence of density and viscosity of vegetable oils. Biomass Bioenergy. **42**, 164–171 (2012)
Gaurav, A., Leite, M.L., Ng, F.T.T., Rempel, G.L.: Transesterification of triglyceride to fatty acid alkyl esters (biodiesel): comparison of utility requirements and capital costs between reaction separation and catalytic distillation configurations. Energy Fuel. **27**, 6847–6857 (2013)
Gülüm, M.: Experimental investigation of the effect of various production parameters on the some fuel properties of produced biodiesels from corn and hazelnut oils, Master's Thesis, Karadeniz Technical University, Turkey (2014)
Holman, J.P.: Experimental Methods for Engineers, 7th edn. McGraw-Hill, New York (2001)
Iwasaki, M., Ikeya, N., Itoh, M., Itoh, M., Yamaguchi, H.: Development and evaluation of catalysts to remove NOx from diesel engine exhaust gas, Sae Technical Paper, doi:10.4271/950748 (1995)
Lin, R., Zhu, Y., Tavlarides, L.L.: Effect of thermal decomposition on biodiesel viscosity and cold flow property. Fuel. **117**, 981–988 (2014)
Mejia, J.D., Salgado, N., Orrego, C.E.: Effect of blends of diesel and palm-castor biodiesels on viscosity, cloud point and flash point. Ind. Crop. Prod. **43**, 791–797 (2013)
Moser, B.R.: Biodiesel from alternative oilseed feedstocks: camelina and field pennycress. Biofuels. **3**, 193–209 (2012)
Ozcanli, M., Serin, H., Saribiyik, O.Y., Aydin, K., Serin, S.: Performance and emission studies of castor bean (ricinus communis) oil biodiesel and its blends with diesel fuel. Energy Sources. **34**, 1808–1814 (2012)
Pratas, M.J., Freitas, S.V.D., Oliveira, M.B., Monteiro, S.C., Lima, A.S., Coutinho, J.A.P.: Biodiesel density: experimental measurements and prediction models. Energy Fuel. **25**, 2333–2340 (2011)
Rahimi, M., Aghel, B., Alitabar, M., Sepahvand, A., Ghasempour, H.R.: Optimization of biodiesel production from soybean oil in a microreactor. Energy Convers. Manag. **79**, 599–605 (2014)
Sivanathan, S., Chandran, H.P.: Investigation on the performance and emission characteristics of biodiesel and its blends with oxygenated additives in a diesel engine, Sae Technical Paper, doi:10.4271/2014-01-1261 (2014)
Sivaramakrishnan, K., Ravikumar, P.: Determination of higher heating value of biodiesels. Int. J. Eng. Sci. Technol. **3**, 7981–7987 (2011)
Stalin, N., Prabhu, H.J.: Performance test of IC engine using karanja biodiesel blending with diesel. ARPN J. Eng. Appl. Sci. **2**, 32–34 (2007)
Tong, D., Hu, C., Jiang, K., Li, Y.: Cetane number prediction of biodiesel from the composition of the fatty acid methyl esters. J. Am. Oil Chem. Soc. **88**, 415–423 (2011)
Yuan, W., Hansen, A.C., Zhang, Q., Tan, Z.: Temperature-dependent kinematic viscosity of selected biodiesel fuels and blends with diesel fuel. J. Am. Oil Chem. Soc. **82**, 195–199 (2005)
Yuan, W., Hansen, A.C., Zhang, Q.: Predicting the temperature dependent viscosity of biodiesel fuels. Fuel. **88**, 1120–1126 (2009)
Yuan, W., Hansen, A.C., Zhang, Q.: Predicting the physical properties of biodiesel for combustion modeling. Am. Soc. Agric. Eng. **46**, 1487–1493 (2003)